ELSEVIER

Biophysical Chemistry 59 (1996) 155–170

Biophysical Chemistry

Thermodynamics of the interactions of sanguinarine with DNA: influence of ionic strength and base composition

Anjana Sen, Arghya Ray, Motilal Maiti *

Biophysical Chemistry Laboratory, Indian Institute of Chemical Biology, Calcutta 700032, India

Received 5 June 1995; revised 25 September 1995; accepted 16 October 1995

Abstract

Using a combination of spectrophotometric and spectrofluorimetric techniques, we report the first thermodynamic characterization of sanguinarine binding to a series of natural and synthetic host DNA duplexes over a wide range of temperature and sodium concentration. The binding isotherms fit reasonably well to the neighbour exclusion model. The salt and temperature dependence of the binding constants is used to estimate the thermodynamic parameters involved in the interaction of the alkaloid with DNA. The resulting binding data are found to be sensitive to the ionic strength of the medium, base composition and sequence of base pairs. When the sodium ion concentration is increased from 0.005 M to 0.5 M, the binding free energy changes vary in a range from -8.47 to -7.1 kcal mol^{-1}, which corresponds to a binding constant range from 1.85×10^6 to 1.8×10^5 M^{-1} at 20°C. More distinct is the spread in the binding enthalpy changes which range from -6.35 to -2.62 kcal mol^{-1} corresponding to binding entropy changes from $+7.22$ to $+15.3$ cal K^{-1} mol^{-1} at 20°C. On the other hand when the GC content of the host DNA duplexes is increased, the binding free energy varies in a range from -7.28 to -8.58 kcal mol^{-1} with the binding enthalpy changes ranging from -0.46 to -14.31 kcal mol^{-1}, while corresponding binding entropy changes range from $+23.3$ to -19.56 cal K^{-1} mol^{-1} at 20°C. Sanguinarine binding to natural DNAs and homo- and heteropolymers of AT is characterized by negative enthalpy changes and positive entropy changes, while binding to homo- and heteropolymers of GC is reflected by both negative enthalpy changes and entropy changes. Possible molecular contributions towards sign and magnitude of the thermodynamic parameters and their dependence on ionic strength, base composition and sequences, are discussed.

Keywords: Sanguinarine; DNA; Alkaloid–DNA interactions; Spectrophotometry; Spectrofluorimetry; Thermodynamics

1. Introduction

The study of the interaction of many naturally occurring and synthetic organic ligands with DNA is an active area of research at the interface of chemistry and biology [1–6]. Many of these compounds bind non-covalently to double-stranded DNA duplexes by intercalation, a process in which planar aromatic rings of the compound get inserted between adjacent DNA base pairs. Such compounds are important because of their potential use in the treatment of cancer and other diseases in humans [1,7,8]. These DNA-binding ligands have been studied extensively in a large number of laboratories primarily directed towards understanding of the fundamental binding

* Corresponding author.

SSDI 0301-4622(95)00137-9

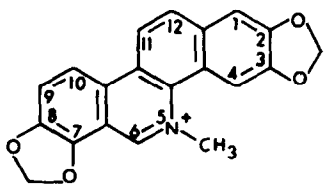

Fig. 1. Chemical structure of sanguinarine iminium form.

equilibria involved, the structure of intercalation complexes and the structural alterations in DNA that result from intercalation [1,2,6,9,11]. It is known that thermodynamic and structural studies are mutually complementary and both are necessary for complete elucidation of the molecular interaction involved in the intercalation site [12–21].

Sanguinarine (Fig. 1), a benzophenanthridine alkaloid, has displayed antimicrobial, antiplaque and antitumour activities [22–25]. Its salt has been used in toothpastes and dental rinses [26]. It exhibits strong anti-inflammatory and anti-tubulin effects [27,28]. It has also been reported to be a phototoxic singlet oxygen [29] and hydrogen peroxide producing alkaloid [30]. Sanguinarine uncouples respiration and oxidative phosphorylation in rat liver mitochondria [31]. It inhibits both photosynthetic phosphorylation associated with ferricyanide reduction and cyclic photophosphorylation catalysed by phenazine methosulphate [32]. Extensive spectrophotometric, spectrofluorimetric, spectropolarimetric, viscometric and other studies show that it forms a molecular complex with various natural and synthetic DNAs exhibiting GC specificity and binds to DNA by a mechanism of intercalation [33–39]. Sanguinarine has pH-dependent structural equilibrium between the iminium form (charged) and the alkanolamine form (neutral) as revealed by spectrophotometry, spectrofluorimetry, high-performance liquid chromatography (HPLC) and NMR spectroscopy [40,41]. Recently, it has been shown that only the iminium form binds to DNA by intercalation and the alkanolamine form does not bind to DNA [42]. To complement the structural data on sanguinarine–DNA interaction, it is necessary to gain an insight into the stability and overall forces of complexation. This approach requires the elucidation of the thermodynamic aspects of binding which we present in this study.

2. Materials and methods

Clostridium perfringens (CP) DNA (type XII, 30 mol% GC), calf thymus (CT) DNA (type I, 42 mol% GC), *Escherichia coli* (EC) strain B DNA (type VII, 50 mol% GC), *Micrococcus lysodeikticus* (ML) DNA (type XI, 72 mol% GC), and synthetic polynucleotides, poly(dA–dT).poly(dA–dT), poly(dG–dC).poly(dG–dC), poly(dA).poly(dT) and poly(dG).poly(dC) were obtained from Sigma (St. Louis, MO) and were tested for their nativeness and purity [11]. Each natural DNA exhibited a characteristic ultraviolet absorption spectrum with an A_{260}/A_{280} ratio between 1.88 and 1.93, and an A_{260}/A_{230} ratio between 2.12 and 2.22. Each polymer concentration was determined spectrophotometrically at the indicated subscripted wavelengths (nm) using the following molar extinction coefficients, ε (M^{-1} cm^{-1}) expressed in terms of DNA phosphates: ε_{260} of CP DNA = 6300, ε_{260} of CT DNA = 6600, ε_{260} of EC DNA = 6500, ε_{257} of ML DNA = 6900, ε_{260} of poly(dA–dT).poly(dA–dT) = 6650, ε_{255} of poly(dG–dC).poly(dG–dC) = 8400, ε_{260} of poly(dA).poly(dT) = 6000, ε_{253} of poly(dG).poly(dC) = 7400. Sanguinarine chloride was purchased from Aldrich (Milwaukee, WI) and was used after checking its purity by thin-layer chromatography and melting point, and also characterizing by mass spectrometry and NMR spectrometry. The alkaloid solution was freshly prepared by dissolving in triple distilled water and was kept protected in dark to prevent any light-induced changes. The drug concentration was determined spectrophotometrically by using a molar extinction coefficient (ε) of 30700 M^{-1} cm^{-1} at 327 nm in 0.1 M HCl as described earlier [43]. The alkaloid obeyed Beer's law in the concentration range used in this study.

DNA binding experiments were performed in citrate–phosphate–EDTA (CPE) buffer (0.982 mM citric acid monohydrate, 2.25 mM purified anhydrous Na_2HPO_4, 0.25 mM EDTA, pH 5.2 ± 0.01) and different sodium concentrations were obtained by adding required volumes of sodium chloride solution from a known concentrated stock. It has been observed that the physico-chemical properties of four natural DNAs and four synthetic polynucleotide duplex DNAs remained unchanged in the CPE buffer

pH 5.2 as evidenced from absorption spectroscopy and circular dichroism studies [44]. The pH was measured with an EC digital pH meter (PH 5652A, Electronics Corporation, India) with an accuracy of 0.01. Glass distilled deionized water and analytical grade reagents were used throughout.

2.1. Spectrophotometric measurements

The absorption spectra of sanguinarine mixed with or without DNA were obtained using a Shimadzu Model UV-260 UV–VIS automatic recording double-beam spectrophotometer (Shimadzu, Japan) against an appropriately prepared reference or control in a quartz cell of 1 cm path-length. The spectrophotometric titrations were performed by keeping the concentration of sanguinarine constant while varying the DNA concentration as described [10,33].

2.2. Temperature-dependent spectrophotometry

These measurements were performed at 15, 20, 30 and 40°C either by a complete titration at a constant temperature or by increasing the temperature of a sample containing a fixed ratio of alkaloid/DNA (D/P), allowing an equilibrium period of 5 min before each spectrum was recorded as described [15]. Temperature-dependent spectra were recorded by using a Shimadzu UV-260 double-beam spectrophotometer equipped with a thermoelectric cell temperature programmer (KPC 5) and temperature controller (S-260/SPR-5).

2.3. Spectrofluorimetric measurements

The fluorescence spectra were recorded with a Hitachi F4010 spectrofluorimeter (Hitachi, Tokyo) as described earlier [34]. Temperature-dependent fluorescence spectra were obtained by using a thermoelectric temperature controller Model EYELA unicool UC-55 (Tokyo Rikakikai).

2.4. Calculation of binding parameters

The spectrophotometric titration data at 327 nm (absorption maximum) and spectrofluorimetric titra-

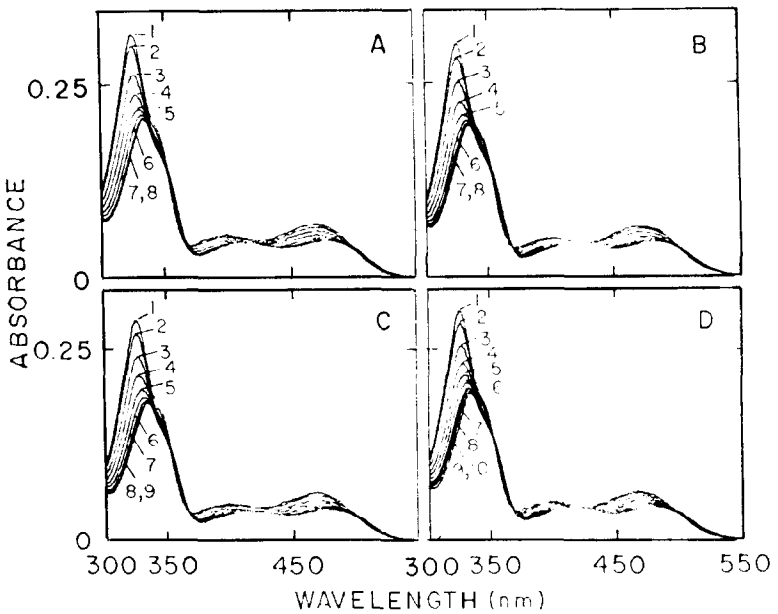

Fig. 2. Absorption spectra of sanguinarine (9.86 μM, curve 1) treated with ML DNA of concentration (A) 4.9, 12.8, 26.6, 39.4, 56.2, 64.1 and 75.5 μM at 15°C denoted by curves (2–8), (B) 4.9, 12.8, 26.6, 39.4, 56.2, 69.0 and 78.9 μM at 20°C denoted by curves (2–8), (C) 4.9, 12.8, 26.6, 39.4, 56.2, 69.0, 81.1 and 93.7 μM at 30°C denoted by curves (2–9) and (D) 4.9, 12.8, 26.6, 39.4, 56.2, 75.0, 83.8, 92.6 and 110.4 μM at 40°C denoted by curves (2–10), respectively. Titrations were performed in CPE buffer with $[Na^+] = 0.02$ M, pH 5.2 ± 0.01.

tion data at 577 nm (emission maximum) against various P/D values were cast into Scatchard plots of r/C_f versus r [45], where r is the number of moles of ligand bound per mole of nucleotide and C_f is the concentration of free ligand. These experimental data were fitted to the neighbour exclusion model of McGhee and Von Hippel [46] for non-cooperative binding according to the following equation:

$$r/C_f = K'(1-nr)[(1-nr)/(1-(n-1)r)]^{n-1} \quad (1)$$

where K' and n represent the intrinsic binding constant to an isolated site and the exclusion parameter, respectively.

2.5. Calculation of thermodynamic parameters

The values of K' and n were determined as described above, at 15, 20, 30 and 40°C for various sodium concentrations. Thermodynamic parameters were estimated by the analysis of the Van't Hoff plot ($\ln K'$ versus $1/T$) obtained over the temperature range of study. The slope of the plot gives the binding enthalpy change ($\Delta H°$) as

$$\delta(\ln K')/\delta(1/T) = -\Delta H°/R \quad (2)$$

The Gibbs free energy change ($\Delta G°$) was determined from the binding constant at a particular temperature according to the relation

$$\Delta G° = -RT \ln K' \quad (3)$$

The entropy change ($\Delta S°$) was estimated from the relationship

$$\Delta S° = (\Delta H° - \Delta G°)/T \quad (4)$$

3. Results

3.1. Absorption spectra

Spectrophotometric studies of the sanguinarine–DNA complexation were carried out at different temperatures and sodium concentrations. The effects of progressively increasing concentration of ML

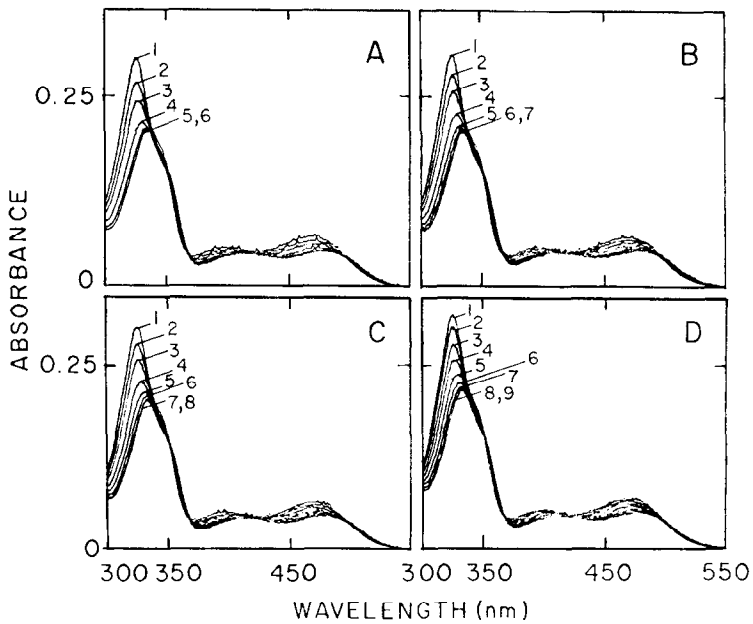

Fig. 3. Absorption spectra of sanguinarine (9.86 μM, curve 1) treated with poly(dG–dC).poly(dG–dC) of concentration (A) 9.8, 19.8, 39.5, 51.3 and 64.1 μM at 15°C denoted by curves (2–6), (B) 9.8, 19.8, 39.5, 51.3, 60.1 and 75.5 μM at 20°C denoted by curves (2–7), (C) 9.8, 19.8, 39.5, 51.3, 60.1, 74.0 and 88.9 μM at 30°C denoted by curves (2–8) and (D) 9.8, 19.8, 29.6, 45.5, 59.2, 74.0, 89.1 and 112.2 μM at 40°C denoted by curves (2–9), respectively. Titrations were performed in CPE buffer with $[Na^+] = 0.02$ M, pH 5.2 ± 0.01.

DNA and poly(dG–dC).poly(dG–dG) on the absorption spectrum of sanguinarine at 15, 20, 30 and 40°C in CPE buffer with a sodium ion concentration of 0.02 M, pH 5.2 ± 0.01, are illustrated in Figs. 2 and 3, respectively. The observed spectral changes essentially involved a gradual red shift and hypochromicity until saturation was reached at each temperature. The spectra exhibit three distinct isosbestic points at 353, 367 and 496 nm in all cases indicating the equilibrium between bound and free alkaloid molecules. Similar features of the spectral changes were observed with all other natural and synthetic DNAs studied.

The effect of sodium ion concentration on the sanguinarine–CT DNA complexation was also studied in CPE buffers with sodium ion concentrations of 0.005, 0.02, 0.05, 0.1 and 0.5 M at different temperatures in each case (not shown). The results show that the hypochromic and bathochromic effects are signif-

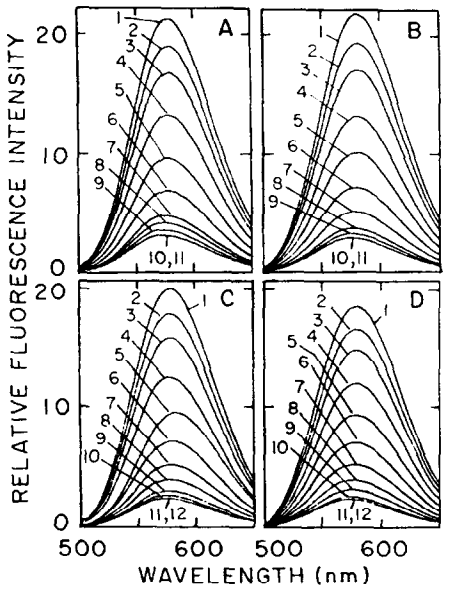

Fig. 4. Fluorescence emission spectra of sanguinarine (9.86 μM, curve 1) treated with ML DNA of concentration (A) 4.9, 9.8, 19.7, 32.5, 49.3, 59.2, 70.0, 78.5, 84.8 and 95.6 μM at 15°C denoted by curves (2–11), (B) 4.9, 9.8, 19.7, 32.5, 49.3, 59.2, 70.0, 78.9, 89.1 and 98.7 μM at 20°C denoted by curves (2–11), (C) 4.9, 9.8, 19.7, 32.5, 49.3, 59.2, 70.0, 78.9, 89.1, 98.7 and 115.3 μM at 30°C denoted by curves (2–12) and (D) 4.9, 9.8, 19.7, 32.5, 49.3, 59.2, 70.0, 78.9, 89.1, 110.5 and 125.4 μM at 40°C denoted by curves (2–12), respectively, in CPE buffer with $[Na^+] = 0.02$ M, pH 5.2 ± 0.01. The excitation was fixed at 475 nm.

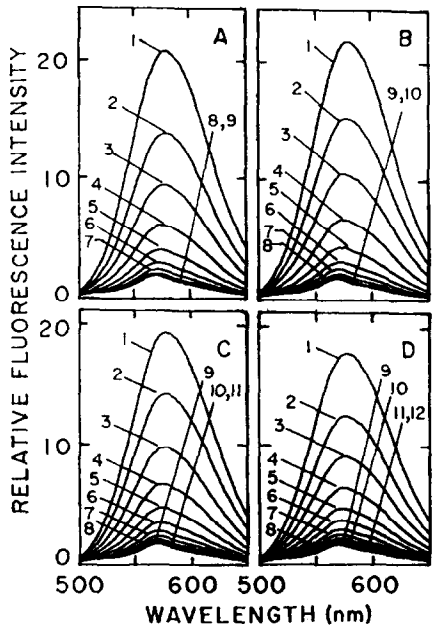

Fig. 5. Fluorescence emission spectra of sanguinarine (9.86 μM, curve 1) treated with poly(dG–dC).poly(dG–dC) of concentration (A) 4.9, 9.8, 17.7, 23.6, 34.5, 39.4, 49.3 and 61.6 μM at 15°C denoted by curves (2–9), (B) 4.9, 9.8, 17.7, 23.6, 34.5, 39.4, 49.3, 59.3 and 69.0 μM at 20°C denoted by curves (2–10), (C) 4.9, 9.8, 17.7, 23.6, 34.5, 39.4, 49.3, 59.3, 75.5 and 83.8 μM at 30°C denoted by curves (2–11) and (D) 4.9, 9.8, 17.7, 23.6, 34.5, 39.4, 49.3, 59.3, 78.0, 89.1 and 110.5 μM at 40°C denoted by curves (2–12), respectively, in CPE buffer with $[Na^+] = 0.02$ M, pH 5.2 ± 0.01. The excitation was fixed at 475 nm.

icantly dependent on temperature and sodium concentration.

3.2. Fluorescence spectra

The fluorescence emission spectrum of sanguinarine when excited at 475 nm showed an emission maximum at 577 nm in the wavelength range of 500–650 nm. We observed a progressive quenching of fluorescence intensity accompanied by a gradual blue shift with increasing concentration of ML DNA and poly(dG–dC).poly(dG–dC) at four different temperatures in CPE buffer with sodium ion concentration of 0.02 M, pH 5.2 ± 0.01, and the resulting spectra are shown in Figs. 4 and 5, respectively. Similar features of spectral changes were observed with all other DNAs except poly(dA–dT).poly(dA–

dT) and poly(dA).poly(dT), where enhancement of fluorescence emission intensity occurred.

Fluorescence spectral characteristics of sanguinarine–CT DNA complexation were also monitored in CPE buffers of various sodium concentrations at four different temperatures (not shown). Here also results display significant dependence on the variation of temperature and sodium concentration.

3.3. Binding parameters

The spectrophotometric titration data (not shown) indicate that the hypochromicity of sanguinarine–DNA complexes are significantly dependent on temperature and salt molarity. The typical binding isotherms are shown in the form of Scatchard plots in Figs. 6 and 7, each of which indicates a non-linear

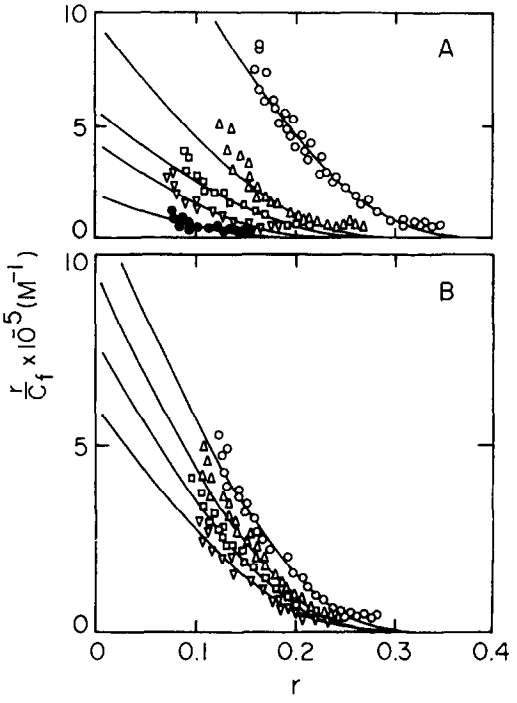

Fig. 6. Representative Scatchard plots for sanguinarine–CT DNA complexation in (A) CPE buffers of varying [Na^+]: 0.005 M (○), 0.02 M (△), 0.05 M (□), 0.1 M (▽) and 0.5 M (●) at 20°C and in (B) CPE buffer of 0.02 M Na^+ at 15°C (○), 20°C (△), 30°C (□) and 40°C (▽). The solid lines are the non-linear least-squares best fit of the experimental points to the neighbour exclusion model (Eq. 1) done on an IBM PC/AT compatible computer. Values of K' and n used to fit Eq. 1 are presented in Table 1.

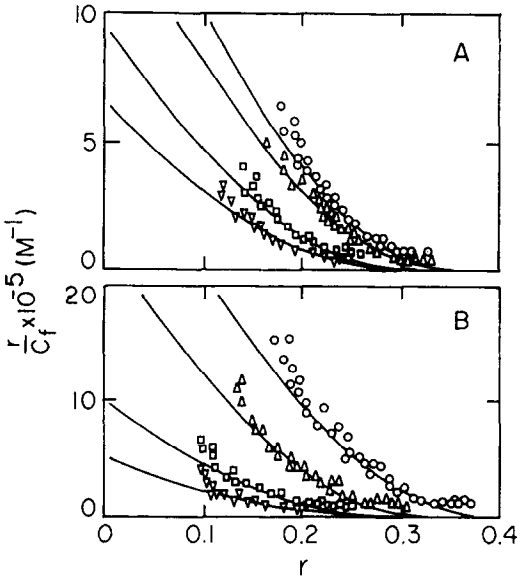

Fig. 7. Representative Scatchard plots for the complexation of sanguinarine with (A) ML DNA and (B) poly(dG–dC).poly(dG–dC) at 15°C (○), 20°C (△), 30°C (□) and 40°C (▽) in CPE buffer of 0.02 M Na^+, pH 5.2±0.01. The experimental data are fitted to Eq. 1 in the same way as done in Fig. 6 and the corresponding best fit values of K' and n used in panel A are presented in Table 2 and those in panel B are given in Table 3.

non-cooperative binding. The Scatchard plots fitted to the neighbour exclusion model (Eq. 1) for the sanguinarine–CT DNA interaction at different sodium concentrations and temperatures are represented in Fig. 6A and B, respectively. The best fit values of the binding parameters K' and n calculated from Eq. 1 used to construct the solid lines in Fig. 6 are presented in Table 1 and these data indicate that the binding constant decreases with increasing temperature and sodium concentration. The ten-fold decrease in K' value and two-fold increase in n value were observed on raising the sodium concentration from 0.005 M to 0.5 M. Again, a two-fold decrease in K' value was observed on raising the temperature from 15 to 40°C, while n values did not change significantly. The binding parameters obtained from spectrofluorimetric titration data under the same conditions are also presented in Table 1. It can be seen from Table 1 that the values of K' and n obtained from two independent methods do not differ significantly.

Table 1
Binding and thermodynamic parameters for the sanguinarine–CT DNA interaction obtained from spectrophotometric (I) and spectrofluorimetric (II) studies [a]

$[Na^+]$ (M)	Temperature (°C)	$K' \times 10^{-5}$ (M^{-1})		n		$\Delta G°$ (20°C) (kcal mol^{-1})		$\Delta H°$ (kcal mol^{-1})		$\Delta S°$ (20°C) (cal K^{-1} mol^{-1})	
		I	II	I	II	I	II	I	II	I	II
0.005	15	23.00 ± 2.0	22.00 ± 2.0	2.70 ± 0.09	2.86 ± 0.09						
	20	18.50 ± 0.9	17.20 ± 0.9	2.73 ± 0.09	2.90 ± 0.10	−8.47 ± 0.08	−8.45 ± 0.08	−6.35 ± 0.14	−6.19 ± 0.14	7.22 ± 0.60	7.70 ± 0.60
	30	13.30 ± 0.7	12.90 ± 0.7	3.30 ± 0.12	3.15 ± 0.12						
	40	10.20 ± 0.5	8.20 ± 0.5	3.41 ± 0.13	3.75 ± 0.14						
0.020	15	11.30 ± 0.7	9.70 ± 0.7	3.20 ± 0.12	3.35 ± 0.12						
	20	9.45 ± 0.5	8.21 ± 0.5	3.43 ± 0.13	3.40 ± 0.13	−8.06 ± 0.08	−8.00 ± 0.08	−5.32 ± 0.12	−5.37 ± 0.12	9.35 ± 0.68	8.99 ± 0.68
	30	7.70 ± 0.4	6.10 ± 0.4	3.47 ± 0.13	3.58 ± 0.14						
	40	6.04 ± 0.4	4.70 ± 0.4	3.50 ± 0.14	3.79 ± 0.14						
0.050	15	6.52 ± 0.4	6.20 ± 0.4	3.45 ± 0.13	3.40 ± 0.13						
	20	5.53 ± 0.3	5.30 ± 0.3	3.60 ± 0.14	3.50 ± 0.14	−7.79 ± 0.07	−7.73 ± 0.07	−4.59 ± 0.11	−4.58 ± 0.11	10.90 ± 0.73	10.76 ± 0.73
	30	4.54 ± 0.3	4.20 ± 0.3	3.70 ± 0.14	3.75 ± 0.14						
	40	3.84 ± 0.2	3.50 ± 0.2	4.24 ± 0.18	3.90 ± 0.17						
0.100	15	4.70 ± 0.3	4.25 ± 0.3	4.05 ± 0.17	3.70 ± 0.14						
	20	4.10 ± 0.3	3.70 ± 0.3	4.20 ± 0.18	4.00 ± 0.17	−7.58 ± 0.07	−7.51 ± 0.07	−3.51 ± 0.09	−3.64 ± 0.09	13.92 ± 0.86	13.19 ± 0.86
	30	3.54 ± 0.2	3.00 ± 0.2	4.39 ± 0.20	4.20 ± 0.18						
	40	2.90 ± 0.2	2.50 ± 0.2	4.80 ± 0.25	5.00 ± 0.25						
0.500	15	1.90 ± 0.2	1.80 ± 0.2	5.12 ± 0.26	3.90 ± 0.17						
	20	1.80 ± 0.1	1.53 ± 0.1	5.20 ± 0.27	4.10 ± 0.18	−7.10 ± 0.06	−7.03 ± 0.06	−2.62 ± 0.07	−2.44 ± 0.07	15.30 ± 0.94	15.69 ± 0.94
	30	1.64 ± 0.1	1.40 ± 0.1	5.35 ± 0.28	4.60 ± 0.24						
	40	1.49 ± 0.1	1.30 ± 0.1	5.50 ± 0.30	5.30 ± 0.28						

[a] Five determinations each.

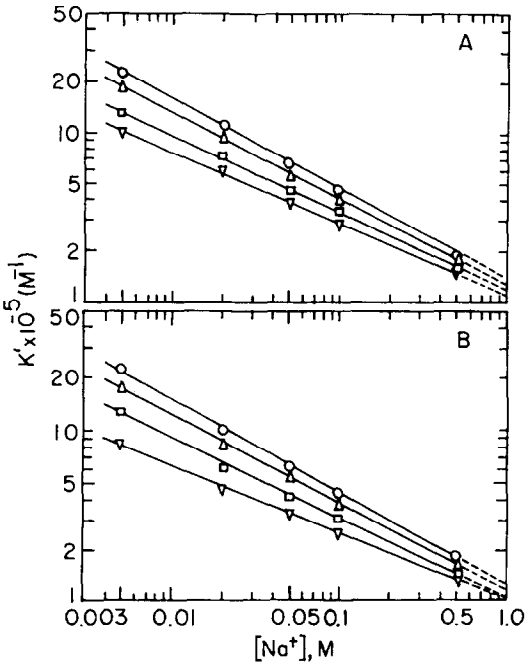

Fig. 8. Dependence of intrinsic binding constant of sanguinarine–CT DNA interaction on ionic strength of the buffer medium at 15°C (○), 20°C (△), 30°C (□) and 40°C (▽) obtained from (A) absorption and (B) fluorescence spectroscopic study (data from Table 1). The data are fitted to straight lines with correlation coefficients ranging from 0.978 to 0.985.

Representative Scatchard plots for the complexation of sanguinarine with ML DNA and with poly(dG–dC).poly(dG–dC) at four different temperatures are illustrated in Fig. 7A and B, respectively. Best fit values of the binding parameters calculated using Eq. 1 from both the spectrophotometric and spectrofluorimetric titration data of the complexation of sanguinarine with four natural and four synthetic DNAs are presented in Tables 2 and 3, respectively.

3.4. Ionic strength dependence

The variation of K' as a function of the molar sodium ion concentration of the buffer medium at four different temperatures is illustrated in Fig. 8. The nature of this relationship has been stated by Record et al. [47] and can be expressed as

$$\ln K' = m'\psi \ln[Na^+] + \ln K'_0 \quad (5)$$

where m' is the effective electric charge of the alkaloid, ψ is the fraction of counterions associated with each DNA phosphate, the quantity $m'\psi$ is the number of counterions released upon binding of a ligand having charge m' and K'_0 is the value of K' at 1 M sodium ion concentration, which is assumed to be a condition free from electrostatic components. For normal double-stranded DNA, $\psi = 0.88$ as proposed by Record et al. [47]. However, considering the intercalation geometry, $\psi = 0.82$ for double-stranded DNA–ligand complex as reported by Wilson and Lopp [48]. The slopes of the straight lines (Fig. 8) indicate release of 0.53, 0.50, 0.46 and 0.41 sodium ions per bound sanguinarine molecule at 15, 20, 30 and 40°C, respectively, as obtained from spectrophotometric studies and 0.55, 0.52, 0.48 and 0.40 from spectrofluorimetric studies. Extrapolation of the data to 1 M sodium ion concentration yields K'_0 values of 1.38×10^5 M^{-1}, 1.27×10^5 M^{-1}, 1.2×10^5 M^{-1} and 1.1×10^5 M^{-1} at 15, 20, 30 and 40°C, respectively, as obtained from spectrophotometric studies and 1.22×10^5 M^{-1}, 1.13×10^5 $^{-1}$, 1.0×10^5 M^{-1} and 1.0×10^5 M^{-1}, from spectrofluorimetric studies. The magnitude of K'_0 indicates the extent to which non-electrostatic forces stabilize the ligand–DNA complex.

3.5. Thermodynamic characterization of sanguinarine–CT DNA complexation

Fig. 9 shows Van't Hoff plots for the temperature-dependent sanguinarine–CT DNA complexation at five different sodium concentrations. The data fits to a straight line for a particular sodium concentration, indicating a small value of heat capacity change [49] in analogy with that observed for other drugs which bind to DNA by intercalation [12–15,18]. The values of thermodynamic parameters evaluated from these plots (Fig. 9) for sanguinarine–CT DNA complexation as a function of sodium concentration are presented in Table 1. It can be seen from Table 1 that enthalpy change and entropy change are significantly dependent on sodium concentration and the binding process is exothermic over the entire range of sodium concentration studied.

The thermodynamic parameters $\Delta G°$, $\Delta H°$ and $\Delta S°$ (Table 1) are plotted as a function of molar sodium ion concentration (Fig. 10). It can be seen

Table 2
Binding and thermodynamic parameters of sanguinarine–natural DNA complexation at $[Na^+] = 20$ mM obtained from spectrophotometric (I) and spectrofluorimetric (II) studies[a]

DNA	Temperature (°C)	$K' \times 10^{-5}$ (M^{-1})		n		$\Delta G°$ (20°C) (kcal mol^{-1})		$\Delta H°$ (kcal mol^{-1})		$\Delta S°$ (20°C) (cal K^{-1} mol^{-1})	
		I	II	I	II	I	II	I	II	I	II
ML	15	17.80 ± 0.9	19.94 ± 0.9	2.80 ± 0.09	3.29 ± 0.12						
	20	14.40 ± 0.8	15.20 ± 0.8	2.85 ± 0.09	3.32 ± 0.12	− 8.30 ± 0.08	− 8.34 ± 0.08	− 7.43 ± 0.16	− 7.53 ± 0.16	3.01 ± 0.45	2.77 ± 0.45
	30	9.52 ± 0.5	9.01 ± 0.5	3.26 ± 0.12	3.40 ± 0.13						
	40	6.48 ± 0.4	7.40 ± 0.4	3.40 ± 0.13	3.55 ± 0.14						
EC	15	13.00 ± 0.7	12.00 ± 0.7	2.85 ± 0.09	3.30 ± 0.12						
	20	10.80 ± 0.6	10.00 ± 0.6	2.94 ± 0.09	3.35 ± 0.12	− 8.14 ± 0.08	− 8.09 ± 0.08	− 6.01 ± 0.14	− 6.07 ± 0.14	7.27 ± 0.60	6.89 ± 0.60
	30	7.80 ± 0.4	7.20 ± 0.4	3.36 ± 0.12	3.50 ± 0.14						
	40	5.69 ± 0.3	5.25 ± 0.3	3.45 ± 0.13	3.65 ± 0.15						
CT	15	11.30 ± 0.7	9.70 ± 0.7	3.20 ± 0.12	3.35 ± 0.12						
	20	9.45 ± 0.5	8.21 ± 0.5	3.43 ± 0.13	3.40 ± 0.13	− 8.06 ± 0.08	− 8.00 ± 0.08	− 5.32 ± 0.12	− 5.37 ± 0.12	9.36 ± 0.68	8.99 + 0.68
	30	7.70 ± 0.4	6.10 ± 0.4	3.47 ± 0.13	3.58 ± 0.14						
	40	6.04 ± 0.4	4.70 ± 0.4	3.50 ± 0.14	3.79 ± 0.16						
CP	15	7.00 ± 0.4	7.00 ± 0.4	3.15 ± 0.11	3.40 ± 0.13						
	20	6.30 ± 0.4	6.30 ± 0.4	3.55 ± 0.14	3.50 ± 0.14	− 7.84 ± 0.07	− 7.82 ± 0.07	− 3.84 ± 0.10	− 3.89 ± 0.10	13.65 ± 0.83	13.40 ± 0.81
	30	5.10 ± 0.4	5.00 ± 0.4	3.65 ± 0.15	3.65 ± 0.15						
	40	4.50 ± 0.4	4.20 ± 0.4	3.80 ± 0.16	3.80 ± 0.16						

[a] Five determinations each.

Table 3
Binding and thermodynamic parameters of sanguinarine–synthetic DNA complexation at $[Na^+] = 20$ mM obtained from spectrophotometric (I) and spectrofluorimetric (II) studies [a]

DNA	Temperature (°C)	$K' \times 10^{-5}$ (M^{-1})		n		$\Delta G°$ (20°C) (kcal mol^{-1})		$\Delta H°$(kcal mol^{-1})		$\Delta S°$(20°C) (cal K^{-1} mol^{-1})	
		I	II	I	II	I	II	I	II	I	II
$[poly(dG-dC)]_2$	15	35.00 ± 3.0	34.45 ± 3.0	2.60 ± 0.08	2.59 ± 0.08						
	20	24.00 ± 2.0	20.00 ± 1.0	3.10 ± 0.10	3.00 ± 0.10	−8.58 ± 0.08	−8.57 ± 0.08	−14.31 ± 0.23	−14.27 ± 0.23	−19.56 ± 0.04	−19.46 ± 0.04
	30	10.00 ± 0.6	10.30 ± 0.6	3.55 ± 0.14	3.50 ± 0.14						
	40	5.00 ± 0.4	6.03 ± 0.4	3.75 ± 0.16	3.85 ± 0.16						
poly dG.poly dC	15	19.00 ± 0.9	19.00 ± 0.9	3.05 ± 0.10	3.02 ± 0.10						
	20	14.50 ± 0.8	12.00 ± 0.7	3.18 ± 0.11	3.10 ± 0.10	−8.28 ± 0.08	−8.27 ± 0.08	−10.86 ± 0.19	−11.17 ± 0.19	−8.83 ± 0.08	−9.78 ± 0.08
	30	7.60 ± 0.4	7.40 ± 0.4	3.60 ± 0.14	3.55 ± 0.14						
	40	4.50 ± 0.4	4.35 ± 0.4	3.95 ± 0.17	3.90 ± 0.17						
$[poly(dA-dT)]_2$	15	4.04 ± 0.3	3.98 ± 0.3	4.35 ± 0.19	4.39 ± 0.19						
	20	3.70 ± 0.3	3.45 ± 0.3	5.00 ± 0.25	4.99 ± 0.25	−7.51 ± 0.07	−7.51 ± 0.07	−2.85 ± 0.08	−2.88 ± 0.08	15.91 ± 0.82	15.82 ± 0.82
	30	3.10 ± 0.3	3.33 ± 0.3	6.00 ± 0.4	6.24 ± 0.40						
	40	2.70 ± 0.2	2.71 ± 0.2	7.50 ± 0.6	7.50 ± 0.60						
poly (dA). poly(dT)	15	2.60 ± 0.2	2.57 ± 0.2	10.00 ± 0.7	9.95 ± 0.70						
	20	2.50 ± 0.2	2.45 ± 0.2	10.50 ± 0.7	10.40 ± 0.70	−7.28 ± 0.06	−7.29 ± 0.06	−0.46 ± 0.03	−0.36 ± 0.03	23.30 ± 0.95	23.65 ± 0.95
	30	2.45 ± 0.2	2.49 ± 0.2	11.50 ± 0.8	10.90 ± 0.80						
	40	2.38 ± 0.2	2.50 ± 0.2	12.20 ± 0.8	11.50 ± 0.80						

[a] Five determinations each.

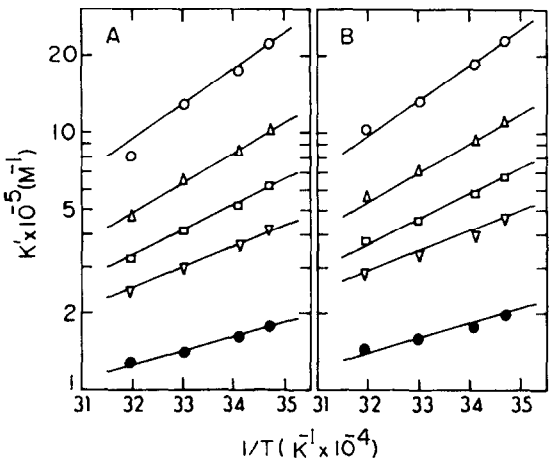

Fig. 9. Van't Hoff plots for sanguinarine–CT DNA complexation in CPE buffers of various [Na^+]: 0.005 M (○), 0.02 M (△), 0.05 M (□), 0.1 M (▽) and 0.5 M (●) as obtained from (A) absorption and (B) fluorescence spectroscopic study (data from Fig. 8). The data are fitted to straight lines with correlation coefficients ranging from 0.965 to 0.99.

from Fig. 10 that there is very little variation in the values of ΔG° with increasing sodium ion concentration while the values of ΔH° and ΔS° vary significantly. Another interesting feature was observed when the data of Table 1 were plotted in terms of ΔH° versus ΔS° as depicted in Fig. 11. The slope of this plot yields a compensation temperature of 436.6 K with a linear correlation coefficient of 0.99 showing an enthalpy–entropy compensatory behaviour similar to other intercalators [12,15–17,50] and oligolysines [49].

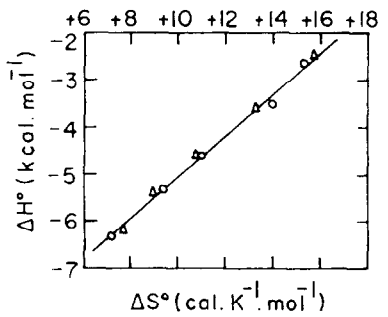

Fig. 11. Plot of enthalpy change (ΔH°) versus entropy change (ΔS°) for sanguinarine–CT DNA complexation in buffers of five different sodium molarities (data from Table 1). The data are fitted to a straight line with slope 436.6 K and correlation coefficient of 0.99. Symbols are same as Fig. 10.

3.6. Influence of base composition and sequence on thermodynamic characteristics

The spectrophotometric and spectrofluorimetric titrations of sanguinarine with eight DNAs were carried out at 15, 20, 30 and 40°C in buffer with a sodium ion concentration of 0.02 M and the binding parameters and thermodynamic parameters are presented in Tables 2 and 3. It can be seen from the tables that the K' value increases with decreasing temperature and increasing GC content, but the n value appears to be almost invariant in case of natural DNAs, while a significant variation of n value was observed for the synthetic polynucleotides of various sequences. Figs. 12 and 13 illustrate the Van't Hoff plots for sanguinarine–natural DNA and

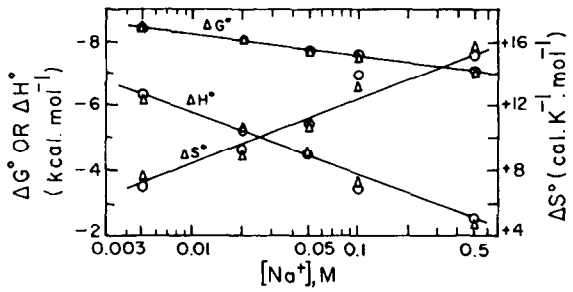

Fig. 10. Dependence of enthalpy change (ΔH°), entropy change (ΔS°) and Gibbs free energy change (ΔG°) for sanguinarine–CT DNA complexation on the ionic strength of the buffer medium, as obtained from absorption (○) and fluorescence (△) spectroscopic study (data from Table 1).

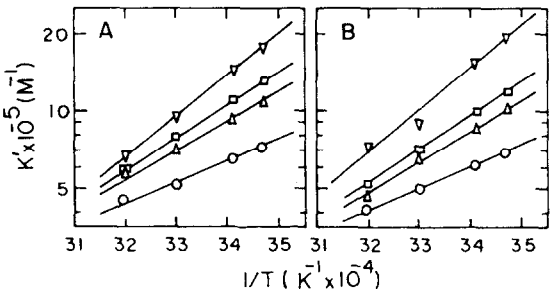

Fig. 12. Van't Hoff plots for the complexation of sanguinarine with ML DNA (▽), EC DNA (□), CT DNA (△) and CP DNA (○) obtained from (A) absorption and (B) fluorescence spectroscopic study (data from Table 2). The data are fitted to straight lines with correlation coefficients ranging from 0.977 to 0.985.

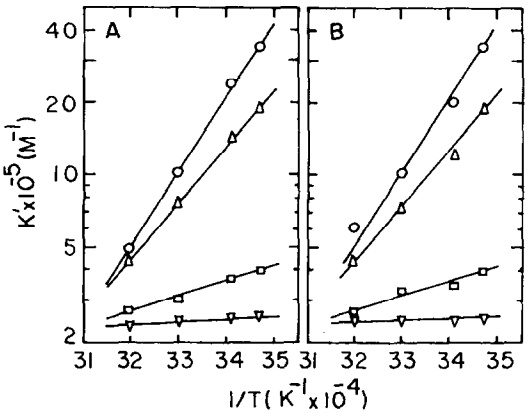

Fig. 13. Van't Hoff plots for the complexation of sanguinarine with poly(dG–dC).poly(dG–dC) (○), poly(dG).poly(dC) (△), poly(dA–dT).poly(dA–dT) (□) and poly(dA).poly(dT) (▽) obtained from (A) absorption and (B) fluorescence spectroscopic study (data from Table 3). The data are fitted to straight lines with correlation coefficients ranging from 0.967 to 0.98.

sanguinarine–synthetic DNA complexation respectively. The linear relationship implies the small values of heat capacity change in each case [49]. Both the enthalpy and entropy change are strong functions of base composition and sequence of base pairs of DNA. Fig. 14 displays a cumulative plot of ΔH° versus ΔS° for all the eight DNAs studied and it, too, retains a linear relationship having a slope of 328 K and correlation coefficient of 0.99. The changes in ΔH° with increasing GC content of DNA are compensated by the changes in ΔS° to produce a relatively small variation in ΔG°.

4. Discussion

The results presented here describe the sanguinarine–DNA interaction over a wide range of temperature, ionic strength, base composition and sequence of base pairs. The interaction is found to be sensitive to these variables. Over the entire range of sodium concentrations studied, sanguinarine binding is exothermic. Both the enthalpy change and entropy change of the binding reaction are strongly dependent on the sodium concentration, base composition and sequence, while the free energy change appears to be less dependent.

4.1. Effects of ionic strength

Sanguinarine is a cationic charged molecule and the electrostatic force may play an important role [51,52]. The importance of electrostatic forces regarding the formation of sanguinarine–DNA complex is emphasized by the results obtained from spectrophotometric and spectrofluorimetric studies. When the ionic strength of the medium is increased, there is a steady decrease in sanguinarine–DNA binding constant. The ten-fold decrease in K' value on raising the ionic strength from 0.005 to 0.5 M

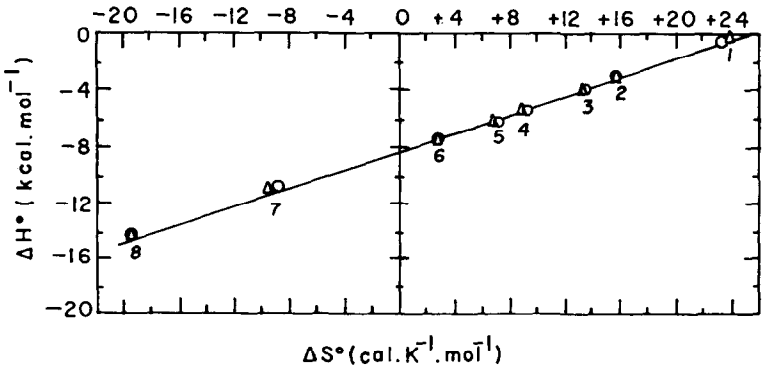

Fig. 14. Plot of enthalpy change (ΔH°) versus entropy change (ΔS°) for the complexation of sanguinarine with (1) poly(dA).poly(dT), (2) poly(dA–dT).poly(dA–dT), (3) CP DNA, (4) CT DNA, (5) EC DNA, (6) ML DNA, (7) poly(dG).poly(dC) and (8) poly(dG–dC).poly(dG–dC) (data from Tables 2 and 3). The data are fitted to a straight line with slope 328 K and correlation coefficient of 0.99. Symbols are same as Fig. 10.

suggests that the electrostatic interaction is not predominant. The fact that binding constant is relatively insensitive to change in ionic strength contrasts with the marked decrease in binding constant with increasing ionic strength detected for other charged intercalating agents [15,16,52,53]. However, it does support that the electrostatic contribution to the binding free energy of the complex must be relatively minor as polyelectrolyte models predict a dependence of the binding constant on the logarithm of the ionic strength for electrostatic interactions [52]. The present data (Table 1 and Fig. 10) conclusively show that the sanguinarine–DNA complex formation possesses a substantial non-electrostatic contribution to their binding free energy. The possibility was considered that the dependence of binding on the ionic strength might be artifactual, perhaps arising from aggregation of alkaloid molecules at higher salt concentrations, but no evidence for such phenomenon was observed in the present study. Moreover, no deviations from Beer's law were noticed over the entire range of sodium ion concentrations studied.

4.2. Thermodynamic characteristics of sanguinarine–DNA complexation

The results of our spectrophotometric and spectrofluorimetric studies at various sodium concentrations and temperatures allowed us to thermodynamically characterize the mode of binding and to define the driving forces behind the binding process. Conceptually, the thermodynamic parameters, free energy, enthalpy and entropy changes, describing the binding reaction, may be determined by the following contributions: (i) the molecular interactions between the bound ligand and the DNA-binding site such as H-bonding, hydrophobic interactions, Van der Waals interactions and electrostatic interactions; (ii) conformational changes either in DNA or in the ligand molecule on complexation, (iii) contributions may come from coupled processes such as ion release, proton release or changes in hydration. The Van't Hoff plots (Figs. 9, 12 and 13) show linear relationship and provide negative enthalpy changes in all cases analogous to that observed for other intercalators [12,15,18]. The values of thermodynamic parameters as a function of sodium concentration (Table 1) reveal that the binding is tending more to an entropy-driven process at higher sodium concentrations. However, the positive entropy changes are in good agreement with prediction [14,47,51] based on modern polyelectrolyte theory, i.e. counterions are released upon binding of cations to the DNA duplex. Again, binding of ligand may directly or indirectly disturb the minor groove [16] and may disrupt the spine of restricted water and release it to bulk solvent. At the highest ionic strength studied here, the contributions of electrostatic forces are negligible and the positive entropy changes suggest the importance of hydrophobicity of the compound in its transfer from bulk solvent to the intercalation site. Thus, it is likely that intercalation of sanguinarine results in a transient base-pair unstacking, disruption of spine of water-structure, alteration of alkaloid–DNA complex, and induces the release of sodium ions thereby increasing the molenumber. All of the above events would contribute to positive entropy change. Similar positive entropic contributions to DNA-binding has been observed for intercalators like ellipticine, actinomycin, proflavin, propidium, ethidium and others [16,18,54].

The plot of Fig. 10 indicates that the large decreases in the enthalpy change observed with increasing salt concentration are being compensated by the increase in the entropy change to produce relatively small change in free energy. The meaning of such enthalpy–entropy compensation [55] is again illustrated in Fig. 11. We have ascertained that our data on compensation behaviour are not artifactual in that the observed compensation temperature of 436.6 K (slope of the line in Fig. 11) is significantly different from the harmonic mean temperature 299 K (i.e. the reciprocal of the average of the reciprocal temperatures expressed in K) at which the data were gathered. The observed enthalpy–entropy compensatory behaviour is similar to that found for other intercalators [12,15–17,50] and oligolysines [49].

The enthalpy changes in sanguinarine–DNA complexation may be explained in terms of the Van der Waals stacking interaction between the benzophenanthrine moiety and the adjacent base pairs, and hydrophobic as well as weak electrostatic interaction. Formation of hydrogen-bonding is not likely in this case, while the entropy changes are due to the release of sodium ions and changes in hydration of DNA duplex structure. It is likely that compensation

behaviour we observed results from fundamental differences in hydration (at levels beyond the minor groove) [56]. A molecular explanation for the reduction in enthalpic and increase in entropic driving forces can be given by two coupled drug-induced solvent effects such as "melting" of hydration layers and release of the "melted" water to the bulk medium. The positive contribution to the binding entropy can be envisioned as an endothermic process, thereby reducing the exothermicity of the intrinsic binding enthalpy change, resulting in enthalpy–entropy compensation. Ionic strength dependence of enthalpy and entropy change, and the enthalpy–entropy compensation are supposed to be a general feature of intercalation reaction [12].

4.3. Base and sequence-dependent thermodynamics

Inspection of thermodynamic data for all the DNAs studied (Tables 2 and 3) reveals that the DNA binding of the alkaloid is an exothermic process and binding to DNAs of higher GC content results primarily from larger negative enthalpy change due to intermolecular interaction at the intercalation site. With all DNAs studied, intercalation is favoured by a negative enthalpy change and is opposed by the positive entropy change except poly(dG–dC).poly(dG–dC) and poly(dG).poly(dC), where the negative enthalpy change is accompanied by negative entropy change. Interestingly, as the GC content decreases, the entropic term increases and dominates by about 2:1 consistent with the results of Schwaller et al. [18]. Over the entire range of GC content, enthalpy changes and entropy changes show a linear relationship; the synthetic polynucleotides (homo- and hetero-) reside on the two extremes of the profile which is conform the results of Breslauer et al. [20]. In all DNAs studied, a relatively small Gibbs free energy change is produced due to the compensatory behaviour of enthalpy and entropy changes. This is judged by the compensation temperature of 328 K (slope of the straight line in Fig. 14) which is significantly higher than the mean harmonic temperature (299 K). A compensation temperature of 328 K strongly suggests binding events where water plays an important role. It is known that DNA undergoes structural transitions upon change in water activity [57]. Recent physico-chemical studies have revealed some intriguing hydration patterns for nucleic acids that appear to depend on base composition, sequence and DNA conformation, all of which represent interrelated properties [57,58]. It was known that B-form DNA is the more hydrated one and AT base pairs are more hydrated than GC pairs [57,59,60]. However, in a very recent study Chalikian et al. [58] showed that water in the hydration shell of GC base pairs is more dense and less compressible than water in the hydration shell of AT base pairs, as revealed from high-precession densimetric and ultrasonic velocimetric measurements suggesting that GC base pairs are solvated more strongly (are more hydrated) than AT base pairs, in contrast with conventional wisdom.

In drug–nucleic acid complexes water molecules add stability by participating in the intermolecular interactions [57,62]. In our study the thermodynamic characteristics of sanguinarine–DNA complexes show that the entropy change increases with decreasing GC content of DNA, reflecting the differential hydration as a function of GC content in these polymers. Again, it has been shown that sanguinarine binds to GC-rich DNA and alternate GC polymer more tightly than AT-rich DNA and alternate AT polymer as revealed from several physico-chemical studies [34–37]. Release of water molecules from the hydration shell of DNA duplex (dehydration of DNA) induced by sanguinarine binding is supposed to make a positive contribution to the value of entropy change. The present data exhibit less dehydration in GC-rich DNA than in AT-rich DNA which is conform the recent observation of Chalikian et al. [58]. The variation of enthalpy and entropy change values shown in Fig. 14 and Table 3 may be correlated with the differences in the hydration properties (perhaps conformation) of both homo- and heteropolymeric duplexes of GC and AT [19,61,62]. The higher entropy change for the poly(dA).poly(dT)–sanguinarine complexation compared with the poly(dA–dT).poly(dA–dT)–sanguinarine complexation is interpreted as due to higher degree of hydration for the latter complex. Thus the differences in the binding of sanguinarine to homo- and heteropolymers of AT reflect differences between the overall hydration and stability of the final state of sanguinarine–DNA complexes rather than the exclusive hydration of initial state of sanguinarine-free homo- and heteropolymeric duplexes. This interpretation is also

applicable to homo- and heteropolymers of GC as well. In our thermodynamic study of poly(dG–dC).poly(dG–dC) and poly(dG).poly(dC), sanguinarine shows a strong enthalpy-driven intercalation process while binding to poly(dA–dT).poly(dA–dT) and poly(dA).poly(dT) is an entropy-driven process, indicating that sanguinarine favours the homo- and heteropolymers of GC for its binding. Wilson and coworkers [63] and Chou et al. [16] have shown the similar entropy-driven process for binding of ethidium and propidium to homo- and heteropolymers of AT duplexes.

5. Conclusions

(1) The complexation of sanguinarine to CT DNA depends on the ionic strength of the medium and the binding is an exothermic process over the entire range of sodium concentrations studied and the binding is tending more to an entropy-driven process towards higher sodium concentrations.

(2) An enthalpy–entropy compensatory behavior is observed in sanguinarine–DNA complexation over the entire range of sodium concentration, base composition and sequence of base pairs studied.

(3) The intermolecular interaction of sanguinarine at the intercalation site of four natural DNAs and two polynucleotides poly(dA–dT).poly(dA–dT) and poly(dA).poly(dT) is characterized by negative enthalpy changes and positive entropy changes, while the complexation with poly(dG–dC).poly(dG–dC) and poly(dG).poly(dC) is reflected by both negative enthalpy and entropy changes.

(4) The enthalpy and entropy changes on complexation of sanguinarine with all DNAs appear to be linearly correlated. These thermodynamic changes reflect the differences in the hydration properties as a function of GC content in natural and synthetic polynucleotide duplexes.

Acknowledgements

A. Sen and A. Ray thank the University Grants Commission, Government of India for the award of Senior Research Fellowship. This work is partially supported by research grants from the Department of Science and Technology (Grant No. SP/SO/D21/91), Government of India.

References

[1] M.J. Waring, Ann. Rev. Biochem., 50 (1981) 159.
[2] H.M. Berman and P.R. Young, Ann. Rev. Biophys. Bioeng., 10 (1981) 87.
[3] P.B. Dervan, Science, 232 (1986) 464.
[4] J.W. Lown, Anti-Cancer Drug Des., 3 (1988) 25.
[5] S. Neidle and Z. Abraham, CRC Crit. Rev. Biochem., 17 (1984) 73.
[6] W.D. Wilson, in M. Blackburn and M. Gait (Eds.), Nucleic Acids in Chemistry and Biology, IRL Press, Oxford, 1989, Chap. 8.
[7] S. Neidle and M.J. Waring, in Topics in Structural and Molecular Biology, Vol. 3, Molecular Aspects of Anti-Cancer Drug Action, MacMillan, London, 1983.
[8] W.B. Pratt and R.W. Ruddon, in The Anti-Cancer Drugs, Oxford University Press, New York, 1979, p. 148.
[9] L.A. Marky, J.G. Snyder, D.P. Remeta and K.J. Breslauer, J. Biomol. Struct. Dyn., 1 (1983) 487.
[10] R. Nandi, S. Chakraborty and M. Maiti, Biochemistry, 30 (1991) 3715.
[11] G.S. Kumar, D. Debnath and M. Maiti, Anti-Cancer Drug Des., 7 (1992) 305.
[12] J.B. Chaires, Biopolymers, 24 (1985) 403.
[13] F. Barcelo, J. Martorell, F. Gavilanes and R.J.M. Gonzalez, Biochem. Pharmacol., 37 (1988) 2133.
[14] A. Bell, J.R. Brown and S. Neidle, Biochem. Pharmacol., 38 (1989) 216.
[15] S. Chakraborty, R. Nandi and M. Maiti, Biochem. Pharmacol., 39 (1990) 1181.
[16] W.Y. Chou, L.A. Marky, D. Zaunczkowski and K.J. Breslauer, J. Biomol. Struct. Dyn., 5 (1987) 345.
[17] G.S. Kumar, D. Debnath, A. Sen and M. Maiti, Biochem. Pharmacol., 46 (1993) 1665.
[18] M.A. Schwaller, G. Dodin and J. Aubard, Biopolymers, 31 (1991) 519.
[19] L.A. Marky and K.J. Breslauer, Proc. Natl. Acad. Sci. USA, 84 (1987) 4359.
[20] D.P. Remeta, C.P. Mudd, R.L. Berger and K.J. Breslauer, Biochemistry, 32 (1993) 5064.
[21] R. Luo, D.T. Braddock, R.M. Subramanian, S.C. Meredith and D.C. Lynn, Biochemistry, 33 (1994) 12367.
[22] V. Preininger, in R.H.F. Manske (Ed.), The Alkaloids, Vol. XV, Academic Press, New York, 1975, p. 207.
[23] G.A. Cordell and N.R. Farnsworth, Lloydia, 40 (1977) 1.
[24] K.S. Kornman, in H. Loe and D.V. Kleinman (Eds.), Proceedings of Dental Plaque Control Workshop, Oxford, 1986, p. 121.
[25] R. Nandi, M. Maiti, K. Chaudhuri, S.B. Mahato and A.K. Bairagi, Experientia, 39 (1983) 524.
[26] R.T. Boulware, G.L. Southard and S.L. Yankell, J. Soc. Cosmet. Chem., 63 (1985) 297.

[27] D. Walterova, J. Ulrichova, V. Preininger and V. Simanek, J. Med. Chem., 24 (1981) 1100.
[28] J. Wolff and L. Knipling, Biochemistry, 32 (1993) 13334.
[29] M. Maiti and A. Chatterjee, Curr. Sci., 68 (1995) 734.
[30] R.W. Tuveson, R.A. Larson, K.A. Marley, G. Wang and M.R. Berenbaum, Photochem. Photobiol., 50 (1989) 733.
[31] M.D. Faddejeva, T.N. Belyaeva, I.P. Novikov, Kh.G. Salabi and A.D. Braun, Dokl. Acad. Nauk. USSR, 253 (1980) 491.
[32] R.H. Vallejos, Biochim. Biophys. Acta, 292 (1973) 193.
[33] M. Maiti, R. Nandi and K. Chaudhuri, FEBS Lett., 142 (1982) 280.
[34] M. Maiti, R. Nandi and K. Chaudhuri, Ind. J. Biochem. Biophys., 21 (1984) 158.
[35] M. Maiti and R. Nandi, J. Biomol. Struct. Dyn., 5 (1987) 159.
[36] R. Nandi, K. Chaudhuri and M. Maiti, Photochem. Photobiol., 42 (1985) 497.
[37] R. Nandi and M. Maiti, Biochem. Pharmacol., 34 (1985) 321.
[38] E. Smekal, N. Kobova and V. Kleinwachter, Stud. Biophys., 101 (1984) 125.
[39] M.D. Faddejeva, T.N. Belyaeva, Yu.M. Rosanev, M. Sedova and E.L. Sokolovskaya, Stud. Biophys., 104 (1984) 267.
[40] M. Maiti, R. Nandi and K. Chaudhuri, Photochem. Photobiol., 38 (1983) 245.
[41] R.R. Jones, R.J. Harkrader and G.L. Southard, J. Nat. Prod. (Lloydia), 49 (1986) 1109.
[42] A. Sen and M. Maiti, Biochem. Pharmacol., 48 (1994) 2097.
[43] A. Das, R. Nandi and M. Maiti, Photochem. Photobiol., 56 (1992) 311.
[44] G.S. Kumar and M. Maiti, J. Biomol. Struct. Dyn., 12 (1994) 183.
[45] G. Scatchard, Ann. NY Acad. Sci., 51 (1949) 660.
[46] J.D. McGhee and P.H. von Hippel, J. Mol. Biol., 86 (1974) 469.
[47] M.T. Record, C.F. Anderson and M. Lohman, Q. Rev. Biophys., 11 (1978) 103.
[48] W.D. Wilson and I.G. Lopp, Biopolymers, 18 (1979) 3025.
[49] D.P. Mascotti and T.M. Lohman, Biochemistry, 32 (1993) 10568.
[50] K.J. Breslauer, D.P. Remeta, W.-Y. Chou, R. Ferrante, J. Curry, D. Zaunczkowski, J.G. Snyder and L.A. Marky, Proc. Natl. Acad. Sci. USA, 84 (1987) 8922.
[51] R.A.G. Friedman, G.S. Manning and M.A. Shahin, in N.R. Kallenbach (Ed.), Chemistry and Physics of DNA-Ligand Interactions, Adenine Press, New York, 1988, p. 37 and references therein.
[52] G. Löber, J. Lumin., 22 (1981) 221.
[53] J.A. Patcher, C.H. Huang, V.H. Du Verney Jr., A.W. Prestayko and S.T. Crooke, Biochemistry, 21 (1982) 1541.
[54] R.M. Wadkins and D.E. Graves, Nucl. Acids Res., 17 (1989) 9933.
[55] R. Lumry and S. Rajender, Biopolymers, 9 (1970) 1125.
[56] B. Lee, Biophys. Chem., 51 (1994) 271.
[57] E. Westhof, Ann. Rev. Biophys. Biophys. Chem., 17 (1988) 125 and references therein.
[58] T.V. Chalikian, A.P. Sarvazyan, G.E. Plum and K.J. Breslauer, Biochemistry, 33 (1994) 2394.
[59] V.A. Buckin, B.I., Kankiya, A.P. Sarvazyan and H. Uedaira, Nucl. Acids Res., 17 (1989) 4189.
[60] V.A. Buckin, B.I., Kankiya, D. Rentzeperis and L.A. Marky, J. Am. Chem. Soc., 116 (1994) 9423.
[61] M.L. Kopka, C. Yoon, D. Goodsell, P. Pjura and R.E. Dickerson, Proc. Natl. Acad. Sci. USA, 82 (1985) 1376.
[62] T.V. Chalikian, G.E. Plum, A.P. Sarvazyan and K.J. Breslauer, Biochemistry, 33 (1994) 8629.
[63] W.D. Wilson, Y.H. Wang, C.R. Krishnamoorthy and J.C. Smith, Biochemistry, 24 (1985) 3991.